Propagation of single-cycle terahertz pulses in random media

Jeremy Pearce and Daniel M. Mittleman

Department of Electrical and Computer Engineering, MS 366, Rice University, Houston, Texas 77251-1892

Received July 13, 2001

We describe what are to our knowledge the first measurements of the propagation of coherent, single-cycle pulses of terahertz radiation in a scattering medium. By measuring the transmission as a function of the length L of the medium, we extract the scattering mean free path $l_s(\omega)$ over a broad bandwidth. We observe variations in l_s ranging over nearly 2 orders of magnitude and covering the entire thin sample regime from $L/l_s \ll 1$ to $L/l_s \sim 10$. We also observe scattering-induced dispersive effects, which can be attributed to the additional path traveled by photons scattered at small angles.

OCIS codes: 290.7050, 300.6270.

The propagation of classical waves in the presence of scattering is a topic of considerable interest in many research communities. In particular, scattering of electromagnetic waves can lead to a rich array of phenomena.[1,2] If the scattering probability is high enough, localization effects analogous to the Anderson localization of electrons can occur,[3] although the unambiguous experimental realization of this effect is quite challenging.[4] With weaker scattering, diffusive transport of photons has been observed.[5,6] This recently prompted a great deal of interest in the medical optics community, as one may hope to image the location of objects immersed in scattering media such as tissue.[7] The usual description of diffusive propagation relies on the fact that the thickness of the sample (L) is much larger than the Boltzmann transport mean free path (l_{tr}).[1] In this case the incident, coherent light beam is completely randomized, and only multiply scattered photons are transported through the sample. As the sample thickness decreases, there must eventually be a crossover from diffusive to ballistic transport.[8] Despite several recent studies of this phenomenon, there are conflicting reports as to the nature of this crossover, and even the value of L/l_{tr} at which it occurs.[9–13]

Here, we describe a new experimental technique for studying the propagation of waves in scattering media and apply it to the investigation of thin samples, for which $L/l_{\mathrm{tr}} < 10$. The measurements are based on terahertz (THz) time-domain spectroscopy, in which broadband single-cycle pulses of free-space THz radiation are generated and coherently detected by use of ultrafast photoconductive sampling.[14,15] This technique offers several unique advantages over other methods used to study multiple-scattering phenomena. First, the results are easier to interpret because the samples are extremely well controlled, and the refractive index and residual absorption coefficient are both known accurately. Difficulty in characterizing the samples has been one of the most significant problems in interpreting experimental results.[4,13] Second, the broad bandwidth of the THz radiation permits the observation of mean free paths ranging over nearly 2 orders of magnitude within the pulse spectrum. This broad bandwidth permits the characterization of a full range of behavior from $L \ll l_{\mathrm{tr}}$ to $L > l_{\mathrm{tr}}$ in a single measurement. Finally, because the technique permits the direct measurement of the spectral phase of the transmitted radiation, a great deal of additional information is available. This capability also proved useful in recent microwave measurements, except that with free-space THz measurements one can avoid the need for a waveguide geometry, which can introduce multimode propagation effects and other complications.[8]

A basic measurement in the study of scattering phenomena is that of transmission through a random medium, as a function of the length of the medium. We construct a model random medium, using commercially available polytetrafluoroethylene (PTFE, or Teflon) spheres, with a size polydispersity of $<3\%$ on the diameter. Teflon is an excellent material for these studies since its absorption coefficient is quite low: $\alpha < 0.1\ \mathrm{cm}^{-1}$ for frequencies below 500 GHz and $\alpha \sim 0.5\ \mathrm{cm}^{-1}$ at 1 THz.[16] Also, the refractive index of Teflon, $n_{\mathrm{PTFE}} = 1.4330$, is nearly independent of frequency throughout the spectral range of the measurements.[16] We have studied spheres of 0.794-mm diameter and also performed a more limited number of measurements on 1.19-mm-diameter spheres. The spheres are contained in a Teflon sample cell, with windows a fixed distance apart. To perform length-dependent studies, we have fabricated 50 such cells, with internal path lengths ranging from 1.19 to 20.64 mm. For each path length, we collect both a reference (empty cell) and a sample waveform, so shifts in the transmission as a result of small variations in the cell-window thicknesses can be corrected.

The subpicosecond THz pulses are generated and detected with a setup quite similar to the one described by Mittleman *et al.*,[17] except that $f = 10$ cm polyethylene lenses are used instead of off-axis paraboloidal reflectors to transport the THz beam, as shown in Fig. 1. The confocal parameter for our optical configuration is at least ten times the sample thickness, so the beam approximates a plane wave in the medium. Figure 2(a) shows a series of waveforms for several different path lengths. As the path length increases, the pulse takes longer to propagate through the sample, and its amplitude decreases. This decrease is due primarily to the scattering of high-frequency components, as can be seen in Fig. 2(b). The low-frequency portions of the waveform scatter much less readily and therefore persist to much longer path lengths. Also, as can be

0146-9592/01/242002-03$15.00/0

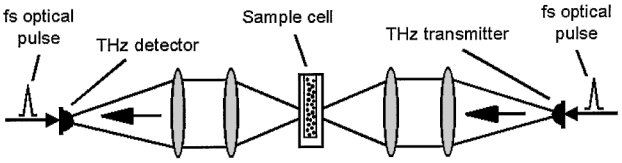

Fig. 1. Schematic of the transmission experiment.

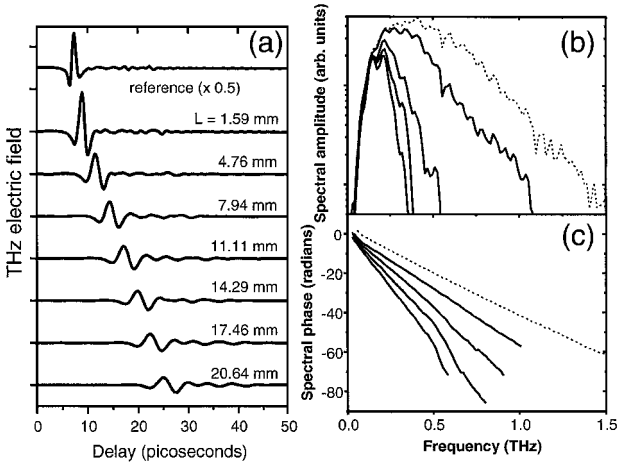

Fig. 2. (a) THz waveforms transmitted through a random medium consisting of a collection of Teflon spheres. Path lengths are as shown. The reference waveform has been reduced in amplitude by a factor of 2. Each vertical tick mark is 1 nA. (b) Amplitudes and (c) phases of the Fourier transforms of the reference waveform (dashed lines), and the first, third, fifth, and seventh waveforms in (a).

seen in Fig. 2(c), the spectral phase shows slightly nonlinear behavior as the path length increases.

The results of Fig. 2(b) can be understood as the frequency-dependent scattering of photons out of the coherent beam. The transmission of the coherent beam varies exponentially with propagation distance according to $|E_{\mathrm{coh}}(\omega)| = \exp[-z/2l_s(\omega)]\exp[-\alpha(\omega)z/2]|E_{\mathrm{in}}(\omega)|$, where $l_s(\omega)$ is the scattering mean free path, related to the transport mean free path by $l_{\mathrm{tr}}/l_s = 1/(1 - \langle\cos\theta\rangle)$.[1] The measured values of $l_s(\omega)$ are shown in Fig. 3 for the two different sphere diameters. Including the absorption factor, $\alpha(\omega)$, shifts the estimated mean free path by no more than 5%, so it is neglected in the determination of these results. The more limited data set for the larger diameter is due to the limited availability of these spheres; nevertheless, it is clear that these larger spheres have a distinctly smaller mean free path. For the smaller spheres, l_s varies from $\sim$1 to $\sim$70 mm across the measurable spectrum. Using these results, we calculate values of kl_s ranging from $\sim$20 to 160 (inset of Fig. 3). This confirms that, with a small dielectric contrast, one is always in the weak scattering limit, $kl_s \gg 1$.

Because these samples are composed of nearly ideal spheres, it is possible to compare the results shown in Fig. 3 with Mie theory, which can be used to compute the scattering cross section σ_s for an isolated dielectric sphere. Indeed, this formalism was recently applied to scattering of THz pulses from isolated spheres.[18,19] Although the applicability of Mie theory to dense collections of spheres is not clear, it is nonetheless instructive to compare its predictions with our results. The solid curve in Fig. 3 shows a numerical computation of $l_s(\omega) = [n_0\sigma_s(\omega)]^{-1}$ for the smaller spheres by use of Mie theory. Here n_0 is the number density of spheres, which we can determine by weighting the cell on a precision balance. From such measurements we determine a volume fraction of $\phi = 0.56 \pm 0.04$ and therefore a number density of $n_0 = 2.14 \pm 0.15$ spheres/mm^3. Except at the shortest wavelengths, the Mie result is significantly smaller than the measured values. However, the weak oscillatory structure in the calculated curve is echoed in the data. The departure from Mie theory is probably due to the high volume fraction, which leads to correlations in the sphere positions as a result of excluded volume effects. These are known to increase the mean free path, relative to that predicted by the curve shown in Fig. 3.[20]

In addition to the information available from the amplitude of the transmitted waveforms, we also independently determine the spectral phase [Fig. 2(c)]. This phase can be used to extract an effective refractive index $n_{\mathrm{eff}}(\omega)$ for each path length. The lower solid curve in Fig. 4 shows the average result for all path lengths. In computing this average, we do not include data points for which the amplitude of the THz field is less than twice the noise level. As a result, not all path lengths contribute to the average at each frequency; the error bars show typical uncertainties associated with this averaging procedure. This measurement of n_{eff} can be compared with several different effective medium approximations,[21] including the Maxwell–Garnett rule and volume averaging. Using the known dielectric of Teflon, and neglecting its imaginary part, we can calculate $n_{\mathrm{eff}} = \sqrt{\epsilon_{\mathrm{eff}}}$ for these two cases. The results are shown in Fig. 4.

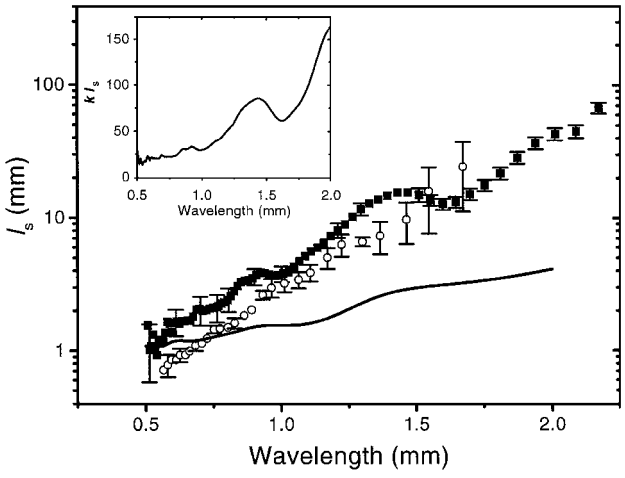

Fig. 3. Scattering mean free path $l_s(\omega)$ versus free-space wavelength, on a log scale. The filled squares are for the smaller spheres, with diameter 0.794 mm, and the open circles are for the larger spheres, $d = 1.19$ mm. The solid curve shows $l_s(\omega)$ for the smaller spheres, computed with Mie theory. The error bars represent the uncertainties associated with repeated measurements. The inset shows the measured values of kl_s versus wavelength for the smaller spheres.

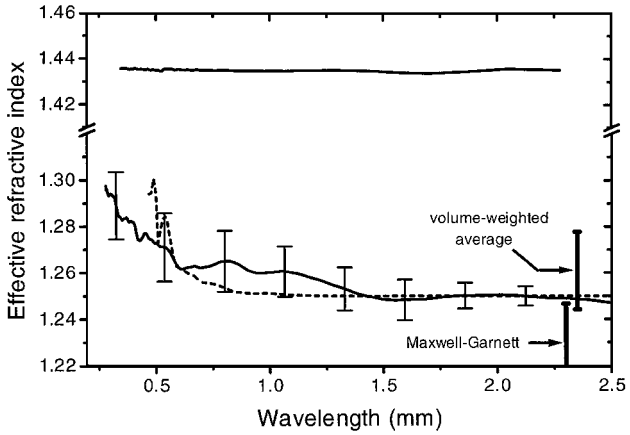

Fig. 4. The bottom solid curve shows the effective refractive index, which exhibits dispersive effects due to scattering. The error bars represent the uncertainties associated with repeated measurements. The dashed curve is the result of a Monte Carlo simulation of the effective index using the measured values of $l_s(\omega)$ (Fig. 2) and the long-wavelength limiting value of $n_{\text{eff}}(\omega)$ as inputs. The arrows show two effective-medium approximations for the composite sample, obtained using the measured volume fraction. The uncertainty in the volume fraction leads to the error bars shown. The top portion of the figure shows the measured index of solid Teflon, which is not dispersive and agrees well with literature values.[16]

Several aspects of this result are worth comment. First, at long wavelengths, at which the scattering is weakest, the index is nondispersive and falls at an intermediate value between the predictions of the two effective-medium approximations. This value reflects the effective index in the absence of scattering and demonstrates the inadequacy of effective-medium approximations in situations in which the filling fraction is near 50%. We also observe that, as the wavelength decreases, the measured index gradually increases, with a fractional shift larger than 3% at the smallest accessible wavelength. This effect is also observed with the larger spheres. To demonstrate that this is not due to intrinsic material dispersion in the sample, we show in the top curve of Fig. 4 the measured values for the index of a solid block of Teflon. The index of the bulk material does not vary by more than 0.1% from its average, which is in excellent agreement with literature values.[16]

The dispersion in $n_{\text{eff}}(\omega)$ is more likely the result of the increased path length traversed by photons that have scattered through small angles. The collection optic used in our measurement is approximately $f/2$, so scattered photons whose propagation has been diverted by less than $\sim 14^\circ$ are still collected by the lens. These photons have traveled a slightly longer path through the material and are therefore delayed somewhat. We can provide support for this explanation with a simple Monte Carlo simulation.[21] For this simulation, we use the measured values for $l_s(\omega)$, and also the long-wavelength limiting value of n_{eff} to convert distance traveled within the sample into transit time. The scattering is assumed to be isotropic. A typical output, shown in Fig. 4 (dashed curve), is reasonably consistent with the measured dispersion. It is worth noting that the average additional travel time is less than 2 ps even at the shortest wavelengths and for the longest sample cell. Unlike in the case of strongly scattering samples,[9] this delay is comparable to or shorter than the duration of the incident pulses. As a result, this effect is readily observable, not in the time-domain waveforms, but only as phase distortions in the frequency domain.

In conclusion, we report what is to our knowledge the first use of terahertz time-domain spectroscopy in the study of propagation of waves in random media. The broad spectral coverage permits simultaneous measurements over a large range of parameters. In addition, the spectral phase distortions provide a sensitive measure of scattering statistics. These measurements should eventually lead to the development of THz imaging techniques analogous to diffuse photon-density wave imaging and also hold promise for photon-localization experiments.

This work was supported in part by the National Science Foundation. D. M. Mittleman's e-mail address is daniel@rice.edu.

References

1. A. Ishimaru, *Wave Propagation and Scattering in Random Media* (Academic, New York, 1978).
2. P. A. Robinson, Philos. Mag. B **80,** 2087 (2000).
3. D. S. Wiersma, P. Bartolini, A. Lagendijk, and R. Righini, Nature **390,** 671 (1997).
4. F. Scheffold, R. Lenke, R. Tweer, and G. Maret, Nature **398,** 206 (1999).
5. R. Graaff and J. J. T. Bosch, Opt. Lett. **25,** 43 (2000).
6. X. Li, D. N. Pattanayak, T. Durduran, J. P. Culver, B. Chance, and A. G. Yodh, Phys. Rev. E **61,** 4295 (2000).
7. D. E. Hyde, T. J. Farrell, M. S. Patterson, and B. C. Wilson, Phys. Med. Biol. **46,** 369 (2001).
8. A. A. Chabanov and A. Z. Genack, Phys. Rev. E **56,** 1338 (1997).
9. R. H. J. Kop, P. de Vries, R. Sprik, and A. Lagendijk, Phys. Rev. Lett. **79,** 4369 (1997).
10. M. Boguñá, J. M. Porrà, and J. Masoliver, Phys. Rev. E **59,** 6517 (1999).
11. S. A. Ramakrishna and N. Kumar, Phys. Rev. E **60,** 1381 (1999).
12. Z. Q. Zhang, I. P. Jones, H. P. Schriemer, J. H. Page, D. A. Weitz, and P. Sheng, Phys. Rev. E **60,** 4843 (1999).
13. J. Gomez Rivas, R. Sprik, A. Lagendijk, L. D. Noordam, and C. W. Rella, Phys. Rev. E **63,** 46613 (2001).
14. P. R. Smith, D. H. Auston, and M. C. Nuss, IEEE J. Quantum Electron. **24,** 255 (1988).
15. M. van Exter and D. Grischkowsky, IEEE Trans. Microwave Theory Tech. **38,** 1684 (1990).
16. J. R. Birch, J. D. Dromey, and J. Lesurf, Infrared Phys. **21,** 225 (1981).
17. D. M. Mittleman, R. H. Jacobsen, and M. C. Nuss, IEEE J. Sel. Top. Quantum Electron. **2,** 679 (1996).
18. R. A. Cheville, R. W. McGowan, and D. Grischkowsky, Phys. Rev. Lett. **80,** 269 (1998).
19. M. T. Reiten, D. Grischkowsky, and R. A. Cheville, Appl. Phys. Lett. **78,** 1146 (2001).
20. S. Fraden and G. Maret, Phys. Rev. Lett. **65,** 512 (1990).
21. M. I. Mishchenko, J. W. Hovenier, and L. D. Travis, *Light Scattering by Nonspherical Particles* (Academic, San Diego, Calif., 2000).